Development of a Multi-Resonant Impact-Driven Energy Harvester (MRI-DEH) for Electrification of Rural Rail Crossings

Mohsen Amjadian, Ph.D.
Principal Investigator
Civil Engineering Department
The University of Texas Rio Grande Valley

Constantine Tarawneh, Ph.D.
Director, UTCRS, Co-Principal Investigator
Mechanical Engineering Department
The University of Texas Rio Grande Valley

Md. Ismail Monsury
Graduate Research Assistant
Civil Engineering Department
The University of Texas Rio Grande Valley

Adamaris Sanchez
Graduate Research Assistant
Mechanical Engineering Department
The University of Texas Rio Grande Valley

A Report on Research Sponsored by

University Transportation Center for Railway Safety (UTCRS)

University of Texas Rio Grande Valley (UTRGV)

September 2025

Technical Report Documentation Page

<table>
<tr><td colspan="2">1. Report No.
UTCRS-UTRGV-M1CY24</td><td colspan="2">2. Government Accession No.</td><td colspan="2">3. Recipient's Catalog No.</td></tr>
<tr><td colspan="4" rowspan="2">4. Title and Subtitle
Development of a Multi-Resonant Impact-Driven Energy Harvester (MRI-DEH) for Electrification of Rural Rail Crossings</td><td colspan="2">5. Report Date
September 30, 2025</td></tr>
<tr><td colspan="2">6. Performing Organization Code
UTCRS-UTRGV</td></tr>
<tr><td colspan="4">7. Author(s)
Mohsen Amjadian, Constantine Tarawneh, Md. Ismail Monsury, Adamaris Sanchez</td><td colspan="2">8. Performing Organization Report No.
UTCRS-UTRGV-M1CY24</td></tr>
<tr><td colspan="4" rowspan="2">9. Performing Organization Name and Address
University Transportation Center for Railway Safety (UTCRS)
The University of Texas Rio Grande Valley (UTRGV)
1201 W. University Dr.
Edinburg, TX 78539</td><td colspan="2">10. Work Unit No. (TRAIS)</td></tr>
<tr><td colspan="2">11. Contract or Grant No.
69A3552348340</td></tr>
<tr><td colspan="4" rowspan="2">12. Sponsoring Agency Name and Address
U.S. Department of Transportation (USDOT)
University Transportation Centers Program
1200 New Jersey Ave. SE
Washington, DC, 20590</td><td colspan="2">13. Type of Report and Period Covered
Project Report
June 1, 2024 – August 31, 2025</td></tr>
<tr><td colspan="2">14. Sponsoring Agency Code
USDOT UTC Program</td></tr>
<tr><td colspan="6">15. Supplementary Notes
Conducted in collaboration with the University of Nebraska-Lincoln (UNL)</td></tr>
<tr><td colspan="6">16. Abstract
This study investigates an electromagnetic energy harvester that utilizes an impact-driven frequency up-conversion mechanism to convert low-frequency vibrations into electrical power. The device consists of a plastic cantilever beam with a copper coil attached at its free end, oscillating between two stationary neodymium magnets. A stopper beneath the resonator induces controlled impacts, increasing stiffness and introducing nonlinear dynamics that broaden the resonance frequency range. A finite element model of a multi-span beam under moving loads was developed to assess acceleration inputs, and subsequently an analytical model of the energy harvester with impact effects is developed to analyze the induced voltage under measured acceleration signals of the multi-span beam, both with and without impact. An experimental prototype is also fabricated to validate the effect of impact on widening the harvester's frequency response across different acceleration intensities. Results show that the impact mechanism increases induced voltage and widens operational bandwidth. Specifically, with a 7 mm impact gap, the maximum voltage improved from 32 mV (no impact) to 43 mV (with impact) at 0.20g acceleration, while the frequency bandwidth expanded by 1 Hz.</td></tr>
<tr><td colspan="3">17. Key Words
Electromagnetic devices; Wideband communication systems; Impact; Nonlinear systems</td><td colspan="3">18. Distribution Statement
This report is available for download from https://www.utrgv.edu/railwaysafety/research/mechanical/index.htm</td></tr>
<tr><td>19. Security Classification (of this report)
None</td><td colspan="2">20. Security Classification (of this page)
None</td><td colspan="2">21. No. of Pages
25</td><td>22. Price</td></tr>
</table>

Table of Contents

List of Figures

List of Tables

List of Abbreviations

AWG	American Wire Gauge
A_g	Peak base acceleration
emf	Electromotive force

FE	Finite Element
K_f	Electromechanical coupling factor
δ_p	Impact gap
PSD	Power spectral density
RC	Reinforced concrete
2D	Two-dimensional
USDOT	U.S. Department of Transportation
UTCRS	University Transportation Center for Railway Safety

Disclaimer

The contents of this report reflect the views of the authors, who are responsible for the facts and the accuracy of the information presented herein. This document is disseminated under the sponsorship of the U.S. Department of Transportation's University Transportation Centers Program, in the interest of information exchange. The U.S. Government assumes no liability for the contents or use thereof.

Acknowledgements

The authors wish to acknowledge the University Transportation Center for Railway Safety (UTCRS) for funding this project under the USDOT UTC Program Grant No. 69A3552348340.

1. Introduction

Energy harvesting is an effective technique for generating electrical power by capturing and utilizing renewable energy sources that are abundant in the environment but often remain untapped (Priya and Inman 2009; Spreemann and Manoli 2012). One promising source of such energy is the kinetic energy from ambient vibrations, particularly from the vibrational energy embedded in transportation infrastructure. For example, rail-bridge systems and their key components, such as rails, ballast, and ties, are often subjected to significant vibrations as trains pass over them which can be harvested as electrical energy (Bosso, Magelli, and Zampieri 2021). Figure 1 illustrates a typical rail-bridge system in the US subjected to the successive loads of a moving train's railcars.

If effectively harvested, this vibrational energy can be converted into electrical power using various types of energy harvesters, such as electromagnetic (Amjadian, Agrawal, and Nassif 2022; Sun et al. 2021; Wang et al. 2021) and piezoelectric (Shan, Kuang, and Zhu 2022; F. Yang et al. 2021) harvesters. In a rail-bridge system, the harvested electrical power can be used to supply electrical power for essential electronic equipment along the tracks, including wireless sensors, trackside signaling systems (Pan, Zuo, and Ahmadian 2022), and communication devices(Hadas et al. 2022). For instance, a standard wireless sensor requires approximately 100 mW of electrical power for operation (Gao et al. 2018), which can be supplied by such energy harvesters. However, electromagnetic energy harvesters offer significant advantages due to their low mechanical damping and minimal reliance on mechanical contacts (i.e., low friction) (Amjadian, Agrawal, and Nassif 2021; Priya and Inman 2009; Roundy, Wright, and Rabaey 2004). Their operation is based on Faraday's law in electromagnetics, which governs the induction of electrical current in moving conductors (Amjadian, Agrawal, Silva, et al. 2022; Amjadian and Agrawal 2017; Amjadian, Agrawal, and Nassif 2022).

The key concept of harvesting electrical power from vibration of a primary structure relies on maintaining resonance between the energy harvester and the primary structure at its dominant frequency (Williams and Yates 1996). However, this method is effective only when the vibration is narrowband and dominated by a single frequency. In contrast, structures that experience a wide range of excitation frequencies, such as rail-bridge systems subjected to moving train loads, typically have a wideband vibration ranging from 5 Hz to 50 Hz (Lu, Mao, and Woodward 2012; Y. B. Yang et al. 2021). For this reason, a narrowband energy harvester might face a significant reduction in its efficiency when mounted on such structures for the purpose of electrical power generation.

Figure 1: Image of the Devon railroad bridge (Malla et al. 2017).

This inefficiency can arise from the challenge of tuning the harvester's resonant frequency to match multiple excitation frequencies, or from frequency deviations that result from operational factors or manufacturing uncertainties or imperfections. To address these limitations, research has increasingly focused on developing wideband harvesters capable of responding to multiple excitation frequencies (Aboulfotoh, Arafa, and Megahed 2013; Zhu, Tudor, and Beeby 2009). Various techniques have been proposed to expand the frequency bandwidth of energy harvesters (Tang, Yang, and Soh 2010), such as frequency-up conversion (Zorlu, Topal, and Külah 2011) and the incorporation of nonlinear stiffness mechanisms with either monostable (Mann and Sims 2009) or bistable effects (Ahmad, Khan, and Khan 2021). Notably, hybrid energy harvesters that combine electromagnetic and piezoelectric mechanisms have attracted significant interest because of their potential to generate substantial amounts of electrical power (Dal Bo, Gardonio, and Turco 2020; Harne 2012; Wang et al. 2015). However, it should be noted that these types of harvesters are complex and often costly to implement.

A simple yet effective technique to widen the frequency bandwidth of an energy harvester is to use an impact mechanism by placing a mechanical stopper near the resonator separated by a small gap. The stiffness of the energy harvester's dynamic system is intermittently altered each time the gap closes. This adjustment allows for a shift in the resonance frequency of the energy harvester, thereby widening its frequency bandwidth. The effects of impact mechanisms on the frequency bandwidth of piezoelectric energy harvesters have been studied by many researchers.

For example, Halim and Park (2014) designed a frequency up-conversion piezoelectric harvester incorporating a flexible beam with a proof mass that contacts a smaller beam resulting in an increase in the bandwidth and efficiency of the energy harvester. The study showed that the energy harvester can generate a peak power output of 734 μW within a frequency range of 7–14.5 Hz (Halim and Park 2014). Xu et al. (2017) designed a hybrid energy harvester that combines piezoelectric and electromagnetic mechanisms utilizing a magnetic resonator to impact a beam with piezoelectric strip. This configuration facilitated frequency up-conversion, enhancing power output and enabling efficient wideband energy harvesting (Xu et al. 2017). In a recent work on electromagnetic energy harvesters, Ouakad et al. (2022) developed a nonlinear impact-based energy harvester incorporating dual resonators. The design leveraged magnetic flux and frequency up-conversion to enhance both bandwidth and generated electrical power. The author demonstrated that configurations using repulsive magnets can exhibit superior performance compared to those using attractive magnets (Ouakad, Al-Harthi, and Bahadur 2022). However, the study lacked experimental observations and proof of the concept.

This study presents a combined numerical and experimental investigation of an electromagnetic energy harvester incorporating a mechanical impact mechanism to widen its frequency bandwidth. The harvester consists of a cantilever beam with a coil attached to its free end, serving as a proof mass, while two adjacent magnets generate the necessary magnetic field. To assess the effect of impact on harvested electrical power, a FE model of a multi-span beam subjected to successive moving loads is developed in COMSOL Multiphysics (version 6.2)(COMSOL v.5.4 2024) to analyze the mid-span acceleration of the multi-span beam at varying speeds of the moving load. Moreover, an analytical model is developed to evaluate the harvester's performance under the measured acceleration signals, both with and without impact. Finally, an experimental prototype is fabricated to validate the impact-induced enhancement of frequency bandwidth across different acceleration intensities.

2. Summary

This report presents the first-year findings from a study exploring the development and testing of an electromagnetic energy harvester designed for wideband power generation. The system employs an impact-driven frequency up-conversion mechanism, where a cantilever beam with an attached copper coil interacts with stationary neodymium magnets. A mechanical stopper

positioned beneath the resonator induces controlled impacts, creating nonlinear dynamic effects that enhance voltage output and broaden the harvester's operational bandwidth.

A FE model of a multi-span beam under moving loads was developed in COMSOL Multiphysics to simulate excitation profile, and subsequently an analytical model of the harvester was developed to evaluate induced voltage under both impact and no-impact scenarios. An experimental prototype was fabricated and tested to validate the effect of impacts in widening the operational frequency bandwidth.

Key findings indicate that introducing impact phenomenon significantly improves performance. With a 7 mm impact gap and 0.20g excitation, the harvester produced a maximum output voltage of 43 mV compared to 32 mV without impact, along with a 1 Hz increase in frequency bandwidth.

The results highlight the critical role of impact effects in improving energy harvesting efficiency and frequency response. Future work will focus on the development of dual and quad resonator energy harvesters to further expand the operational frequency bandwidth.

3. Energy Harvester Design

3.1 Design and Configuration

Figure 2 shows the design of the proposed energy harvester highlighting its key components involved in generating electrical power. The energy harvester includes a flexible cantilever beam, specified by dimensions $L_s \times W_s \times H_s$, which serves as the resonator. As depicted in Figure 2, a thick, square-shaped copper coil with dimensions $L_c \times W_c \times H_c$ is mounted on the free end of the beam. This coil is positioned to move freely between two stationary square-shaped permanent magnets, each with dimensions $L_m \times W_m \times H_m$. These magnets are spaced apart from the coil by an air gap of the size δ_a ensuring that the coil can move without physical contact with them.

The cantilever beam's fixed end is attached to a rigid base, which is subjected to the acceleration signal a(t) resulting from the vibrations of a multi-span beam under a series of successive moving loads at varying speeds. A rigid stopper is placed below the free end of the beam, with an adjustable gap size δ_p to shift its resonant frequency by modifying the impact gap size. Table 1 details the geometrical dimensions and material properties of the energy harvester and its key components. The copper coil is wound with AWG-28 wire, and the thickness of the winding is t_c=0.25 in. The total number of coil turns is estimated to be approximately N_c=400.

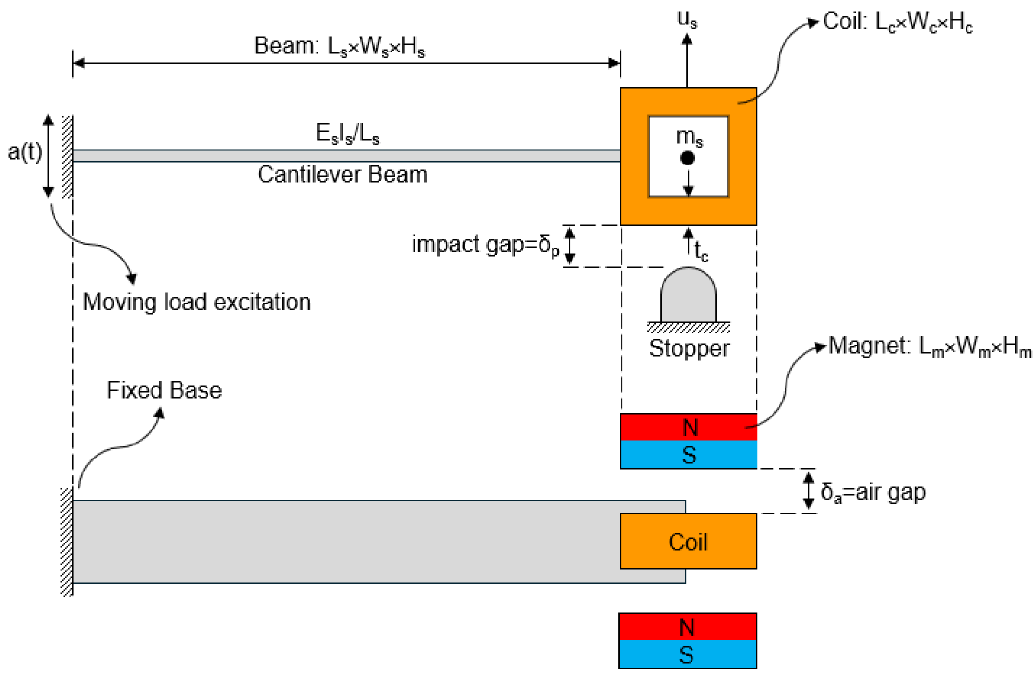

Figure 2: Configuration of the energy harvester and its key components with the stopper mounted below the free end of the cantilever beam.

Table 1: Geometrical dimensions and material properties of the harvester

Parameter	Value	Unit	Description
$L_s \times W_s \times H_s$	6.0×1.0×0.2	in	Beam dimensions
$L_m \times W_m \times H_m$	1.0×1.0×0.125	in	Magnets dimensions
$L_c \times W_c \times H_c$	1.0×1.0×0.5	in	Coil dimensions
t_c	0.125	in	Winding depth of the coil
B_r	1.32	T	Magnetic remanence of the magnets (N42)
d_w	0.0125	in	Diameter of the winding wire
δ_a	0.3	in	Air gap size
δ_p	Var. from 5 to 15	mm	Impact gap size

3.2 Design and Configuration

During an external excitation with the acceleration a(t), the cantilever beam vibrates relative to the base frame and primary structure (i.e., multi-span beam). The applied excitation generates relative velocity between the coil at the beam's free end and the adjacent magnets causing fluctuations in their magnetic flux. According to Faraday's law, these fluctuations induce an electromotive force (emf) within the coil as it moves within the magnetic field of the magnets. When the displacement of the free tip of the beam exceeds the size of the impact gap, an impact occurs, introducing additional stiffness into the dynamic system of the energy harvesters. This mechanism increases the relative velocity between the coil and the magnets, thereby enhancing the electrical power generation. Moreover, the sudden change in stiffness shifts the resonant frequency of the energy harvester, widening its frequency bandwidth. As a result, the proposed energy harvester can operate over a wider frequency range, improving its overall energy harvesting efficiency.

4. Moving Load Analysis

A simplified two-dimensional (2D) FE model is developed using COMSOL Multiphysics (version 6.2)(COMSOL v.5.4 2024) to analyze the response of a multi-span reinforced concrete (RC) beam, functioning as a bridge, under a series of successive moving loads, as shown in Figure 3. The beam is simply supported and has three spans, each measuring 36 m in length (L_{b0}=36 m), 0.5 m in height (H_b=0.5 m), and 1.0 m in width (W_b=1 m). The moving load, representing a series of successive railcars, is simulated through a periodic pulse function. This function has a load intensity of 0.3 MPa and a pulse width of 1 meter (P≈30 tons). The distance between two consecutive pulses is set at 18 meters (S=18 m) which provides a generalized representation of actual spacing between the axles of a typical railcar.

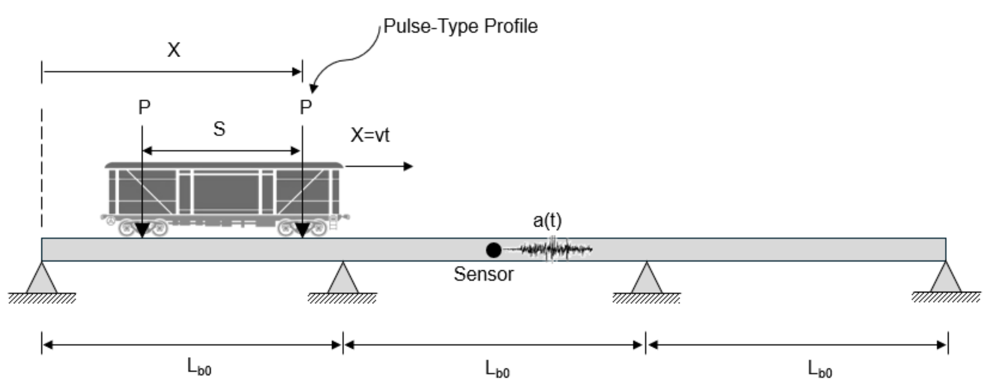

Figure 3: Dynamic model of a three-span RC beam subjected to the successive moving loads of a railcar with two concentrated axle loads.

A time-dependent study is defined in COMSOL to measure the time history of the acceleration of the beam. This study evaluates the time history of acceleration response at the midpoint of the 2nd span of the RC beam. Figure 4a shows this response at various speeds, v=25, 50, and 75 m/s, plotted in terms of the front load's location normalized to total length of the beam. The critical speed of the moving load can be estimated by aligning it with the first mode of vibration of the beam, where the displacement at the midpoint reaches its maximum. This speed is determined by this equation (Frýba 1972):

$$v_{cr} = 2f_1 L_{b0} \tag{1a}$$

where f_1 (=0.58 Hz) is the natural frequency of the first mode, calculated as:

$$f_1 = \frac{\pi}{2}\sqrt{\frac{E_b I_b}{\rho_b A_b L_{b0}^4}} \tag{1b}$$

where $E_b I_b$ denotes the flexural rigidity of the beam, A_b the cross-sectional area, and ρ_b the mass density. By substituting the corresponding values for these parameters into Equation (1), we calculate the critical speed to be v_{cr}=41.5 m/s. Figure 4 also displays the acceleration response at the midpoint of the 2nd span of the RC beam for $v=v_{cr}$. Figure 4b shows the power spectral density (PSD) of the acceleration response in terms of the frequency. In this figure, the effects of moving load on a shift in the resonance frequency of the beam is noticeable.

5. Dynamic Model

5.1 Electromechanical Model

For simplicity, this study focuses only on the first vibration mode of the cantilever beam. Figure 5 illustrates the electromechanical model of the energy harvester, where the mechanical and electrical domains are coupled through the motion of the coil moving within the magnetic field produced by the magnets.

The energy harvesting circuit comprises a coil connected in series to a load which is modeled as a single resistor with electrical resistance R_l. The coil itself is represented by a resistor (R_c) and an inductor (L_c) connected in series, accounting for the coil's resistance and inductance respectively. Electrical power is generated whenever the coil moves relative to the magnets, particularly when it resonates with the base excitation. This relative motion alters the magnetic flux of the magnets passing through the coil, inducing an electromotive force (V_{emf}) in the circuit according to Faraday's law of induction. Consequently, this results in an electric current, $I_{ci}(t)$, flowing through the coil.

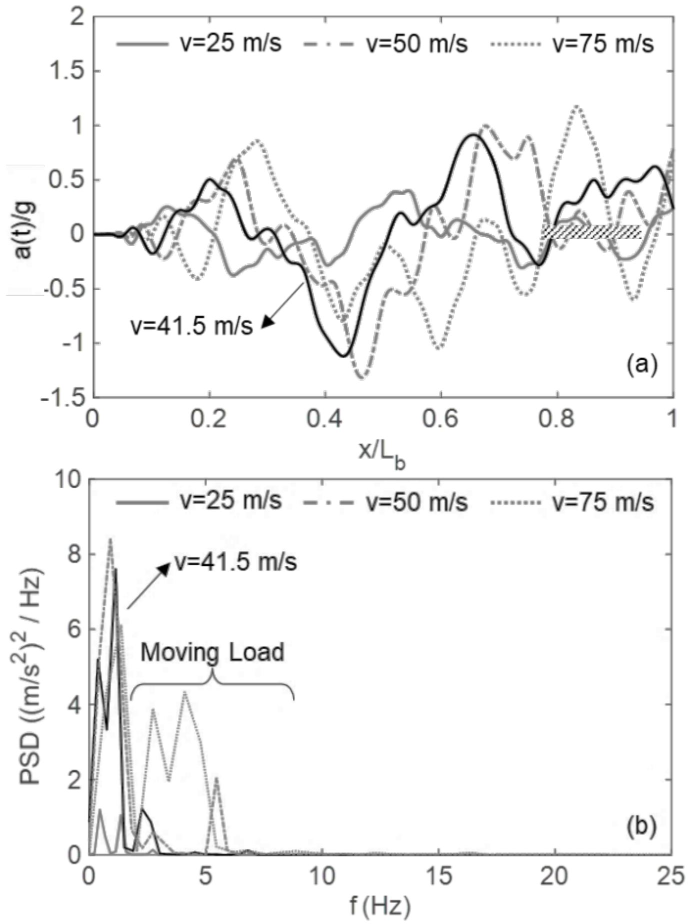

Figure 4: Acceleration response at the midpoint of the 2nd span of the RC beam for the speeds v = 25, 50, 41.5, and 75 m/s (a) plotted in terms of the front load's location normalized to length of the beam with its (b) PSD plotted in terms of frequency

5.2 Governing Equation

The motion of the coil through the magnetic field generated by the magnets, when the cantilever beam is subjected to base acceleration a(t), is modeled by the following coupled differential equations:

$$m_s \frac{d^2 u_s(t)}{dt^2} + c_s \frac{du_s(t)}{dt} + k_s u_s(t) - F_c(t) + F_p(t) = -m_s a(t) \tag{2a}$$

$$L_c \frac{dI_{ci}(t)}{dt} + (R_l + R_c) I_{ci}(t) = V_{emf}(t) \tag{2b}$$

Here, Equation (2a) describes the vibration dynamics of the cantilever beam where $u_s(t)$ represents the displacement of the coil (proof mass), m_s is the proof mass, c_s the mechanical damping coefficient, and k_s the stiffness. The term $F_c(t)$ represents the eddy current damping force acting on the coil, and $F_p(t)$ is the impact force when the impact gap closes, causing the proof mass to collide with the mechanical stopper.

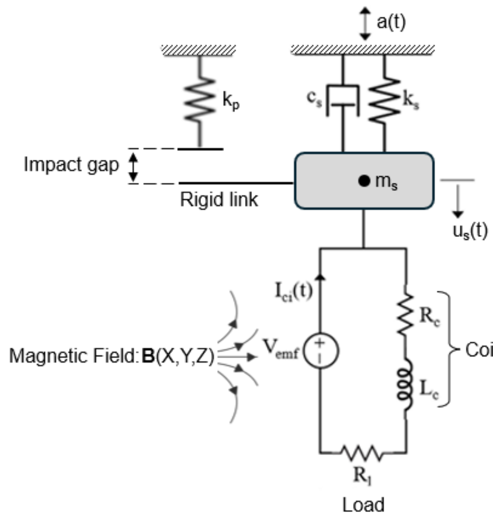

Figure 5: Electromechanical model of the energy harvester with the mechanical stopper modeled as a nonlinear Hertzian spring with stiffness constant kp.

Equation (2b) models the electrical dynamics within the coil where $I_{ci}(t)$ and $V_{emf}(t)$ are the induced current and electromotive force, respectively, generated due to the coil's relative motion with the magnets. The impact force $F_p(t)$, defined in Equation (2a), is modeled using a Hertzian nonlinear spring model:

$$F_p(t) = \begin{cases} k_p \Delta_p(t)^{3/2} & \Delta_p(t) > 0 \\ 0 & \Delta_p(t) \leq 0 \end{cases} \tag{3}$$

where $\Delta_p = -u_s - \delta_p$ is the penetration between the two colliding bodies, and k_p is the stiffness constant of the nonlinear spring. The eddy current damping force, $F_c(t)$, in Equation (2a), is expressed as:

$$F_c(t) = -K_f I_{ci}(t) \tag{4}$$

where K_f is the electromechanical coupling coefficient, assumed constant for simplicity. The induced voltage (i.e., electromotive force) is given by the following expression,

$$V_{emf}(t) = +K_f \dot{u}_s(t) \tag{5}$$

where $\dot{u}_s(t)$ is the velocity of the coil (or the proof mass). Ignoring the effects of L_c from Equation (2b), and integrating Equations (4) and (5) into Equation (2a), the governing equation can be simplified into a decoupled form as follows:

$$\left[1+\frac{33}{140}L_s\right]\ddot{u}_s(t)+4\pi f_s\left[\xi_s+\frac{K_f^2}{4\pi f_s m_s(R_l+R_c)}\right]\dot{u}_s(t)+4\pi^2 f_s^2 u_s(t)+\frac{F_p(t)}{m_s} = -a(t) \tag{6}$$

where f_s represents the natural frequency of the fundamental mode of the cantilever beam, and ξ_s is the critical mechanical damping ratio. It should be also mentioned that the total mass of the resonator has been corrected to include the distributed mass of the cantilever beam. Finally, the performance of the energy harvester is evaluated by using the average value of the instantaneous electrical power generated across the load over the time interval [0,T] which is determined by the following integral (Amjadian, Agrawal, and Nassif 2022),

$$P_{lavg} = \frac{R_l K_f^2}{(R_l+R_c)^2}\left(\frac{1}{T}\int_0^T \dot{u}_s^2(t)dt\right) \tag{7}$$

5.3 Numerical Study

In this section, we present a numerical study to optimize two key design parameters of the energy harvester: the electromechanical coupling factor (K_f) and the impact gap size (δ_p). These parameters influence the efficiency of electrical power generation and the frequency up-conversion mechanism in harvesting power from the vibration of the three-span beam under the given moving load shown in Figure 3. The governing equation, Equation (6), is solved numerically using a block-based modeling technique in Simulink (MATLAB). For this numerical study, it is assumed that m_s=56 gr, k_s=7.9 N/m, c_s=0.068 N.s/m, k_p=25 MN/m, R_c=8.0 Ω, and R_l/R_c=1.0. Figure 6 shows the average harvested power in terms of K_f, ranging from 0 to 15 N/A, for various moving load speeds. The results indicate that the maximum electrical power is achieved at the optimum value K_f=3.1 N/m v=75 m/s, and this optimum value remains nearly the same for other speeds. Figure 7 shows the average harvested power with respect to δ_p, ranging from 0 to 10 cm, for different load speeds under the assumption K_f=3.1 N/m. As the size of impact gap increases, the harvested power rises and then remains constant when there is no impact. The maximum electrical power of approximately 22 mW occurs at δ_p=4.5 cm for v=75 m/s.

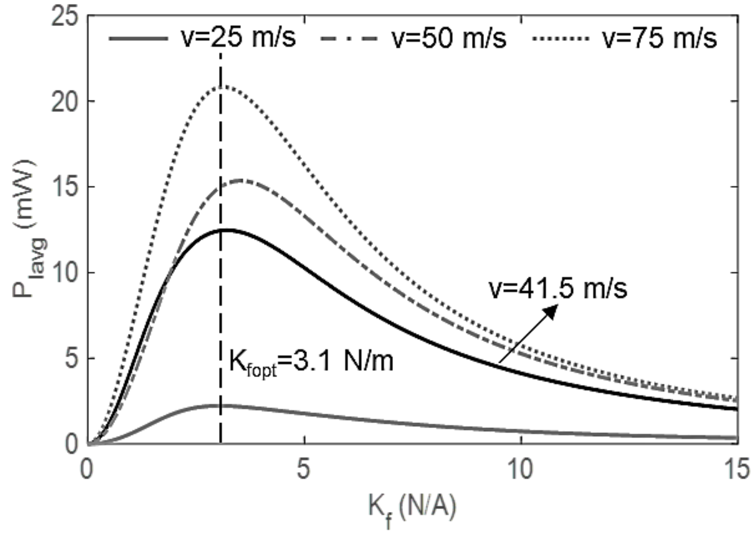

Figure 6: Average harvested power plotted versus the electromechanical coupling factor

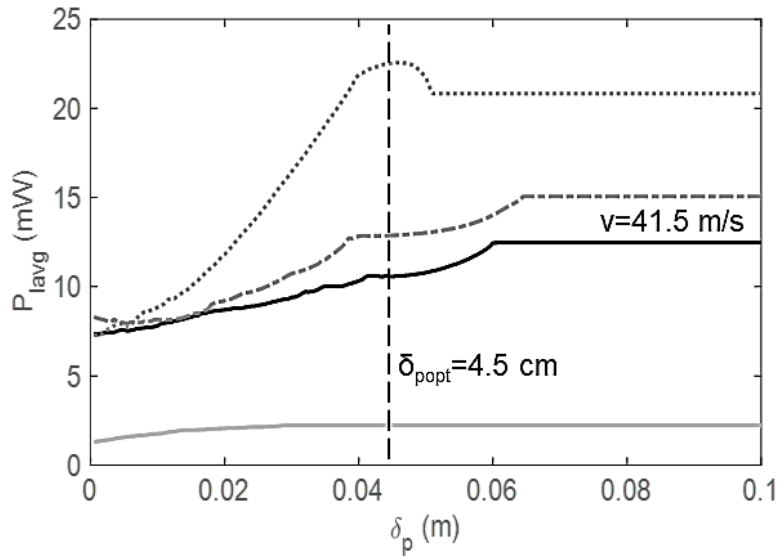

Figure 7: Average harvested power plotted in terms of the impact gap

6. Experimental Study

6.1 Prototype Fabrication and Experimental Setup

Figure 8 displays the prototype of the energy harvester that was fabricated for laboratory testing. The dimensions and material properties of this prototype are aligned with those detailed in

Section 2. Table 1 lists a detailed summary of these properties and geometric specifications used in the fabricated prototype. The key components of the prototype, including the cantilever beam, base frame, and coil holder, were manufactured using a high-quality plastic material (E_b=2 GPa) to ensure durability and consistent performance during testing. To improve the impact stiffness, a stainless-steel screw was utilized as the mechanical stopper. The screw is non-magnetic to prevent interference with the magnetic flux. The setup also includes two magnets on the two sides of the coil where each is screwed to a frame using two vertical slots. These slots allow for the vertical adjustment of the magnets to align their centers precisely with the coil, strengthening the magnetic interaction between the coil and the magnets necessary for efficient energy harvesting.

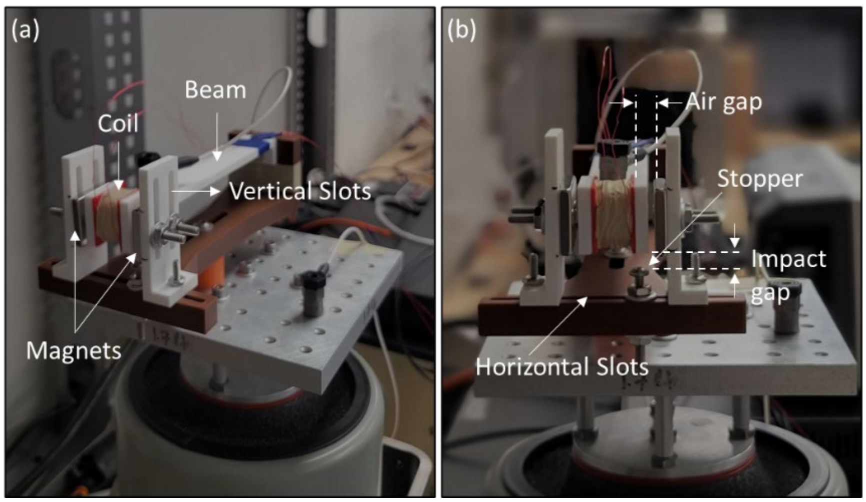

Figure 8: Pictures of the harvester tested in the lab: (a) key components (b) side view of the coil and the mechanical stopper separated by a gap

Figure 9 demonstrates the experimental setup. The prototype is securely fastened to an electrodynamic shaker using a rigid mounting plate. It is subjected to a series of sweeping harmonic excitations within a range of frequencies from 10 Hz to 20 Hz and peak accelerations of 0.15g and 0.20g. Experimental. As designated in Figure 9, Sensor 1 is mounted on the mounting plate to record the input excitation, and Sensor 2 is attached to the free end of the cantilever beam, monitoring the output response and detailing the beam’s vibration dynamics throughout the tests.

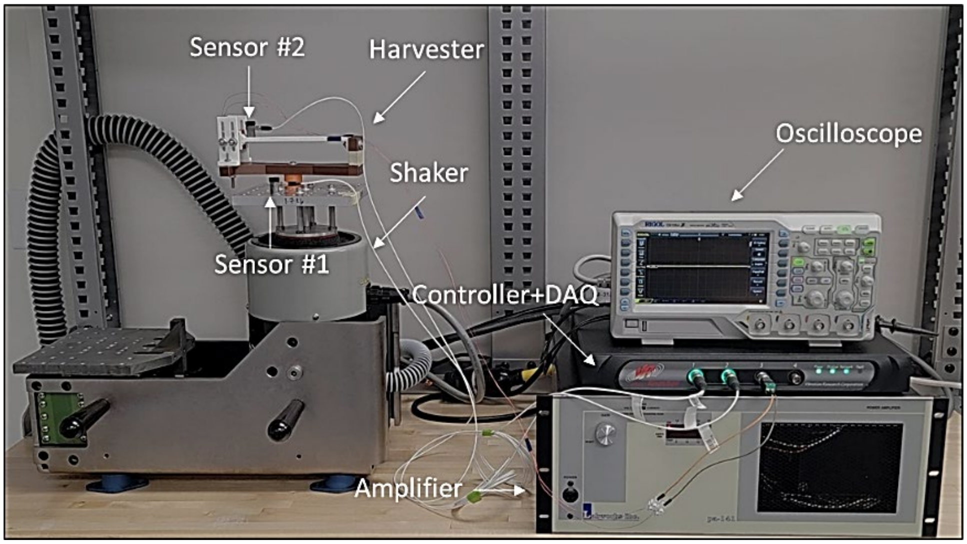

Figure 9: Experimental setup of the harvester in the lab and apparatus used for data measurement

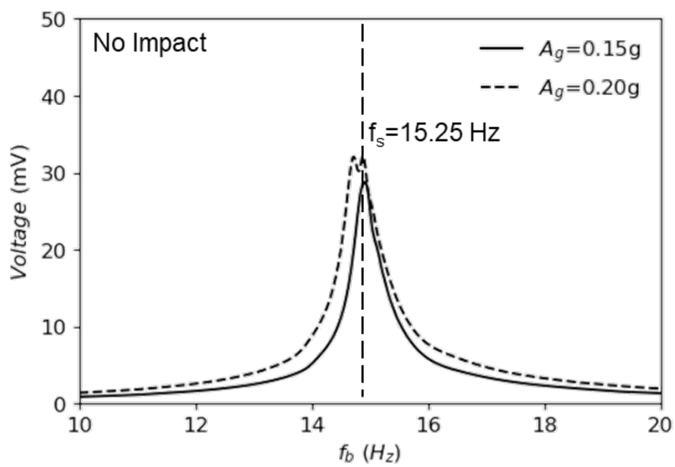

Figure 10: Induced voltage plotted in terms of the excitation frequency without impact, comparing the response for the peak accelerations 0.15g and 0.20g

6.2 Experimental Results

Figure 10 and Figure 11 illustrate the induced voltage in an open-circuit configuration for scenarios with and without impact, respectively. Figure 10 presents the induced voltage in terms of the excitation frequencies ranging from 10 to 20 Hz, for two peak base accelerations of 0.15g and 0.2g. The induced voltage at 0.2g acceleration consistently exceeds that at 0.15g across the frequency spectrum. The resonance frequency is identified at approximately 15.25 Hz, with no significant bandwidth effects observed. At this resonance frequency, the peak voltage recorded for a peak acceleration of 0.15g is approximately 28 mV, while for a peak acceleration of 0.2g, it is about 32 mV.

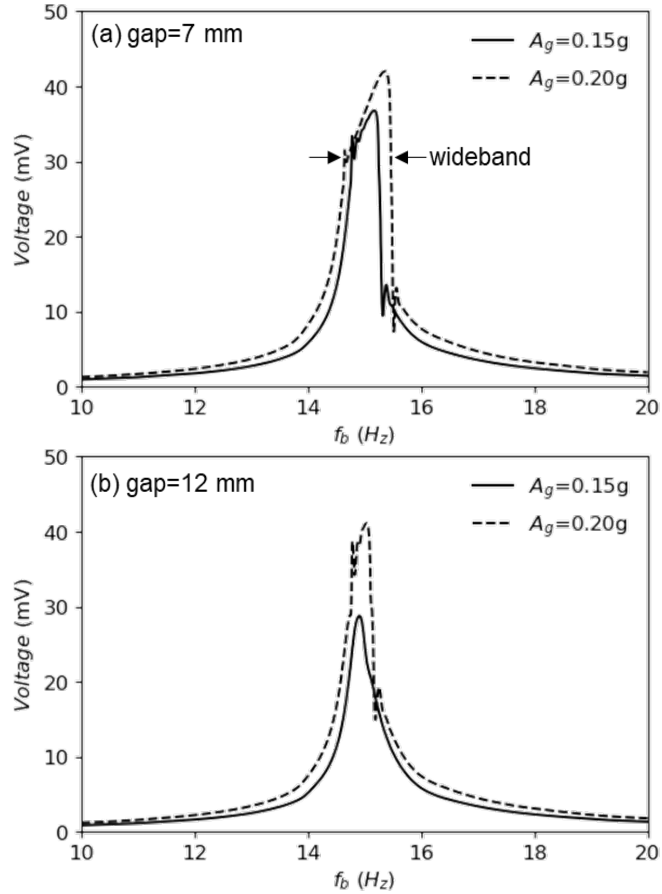

Figure 11: Induced voltage plotted in terms of the excitation frequency with impact, comparing the response for the peak accelerations 0.15g and 0.20g: (a) δp=7 mm; (b) δp=12 mm

Figure 11a and Figure 11b show the plots of the induced voltage in terms of the excitation frequencies ranging from 10 Hz to 20 Hz for contact gaps of δ_p=7 mm and δ_p=12 mm, under two peak base accelerations, 0.15g and 0.2g. As shown in Figure 11a, at a peak acceleration of 0.15g, the deflection of the cantilever beam exceeds the contact gap δ_p=7 mm, triggering an impact between the free end of the cantilever beam and the stopper. This impact widens the resonance bandwidth of the harvester around the resonance frequency of the energy harvester, which is 15.25 Hz. However, when the peak acceleration increases to 0.2g, the bandwidth expands to approximately 1 Hz, ranging from 14.75 Hz to 15.75 Hz for a contact gap of 7 mm. In addition, a noticeable increase in the induced voltage occurs near the resonance frequency, boosting the energy harvester's operational efficiency especially for at the peak acceleration 0.20g, with an increase in output voltage to 43 mV, as depicted in Figure 11a. It is seen that, due to the impact effects, the output voltage exhibits an increase of 11 mV compared to the case without impact as shown in Figure 10. However, when the impact gap (δ_p) is increased to 12 mm, Figure 11b shows that at the peak acceleration 0.15g, the impact has no noticeable effects on the response of the energy harvester. However, upon increasing the peak acceleration to 0.20g, a marginal increase in bandwidth is noted. Despite this, in both cases, the induced voltage decreases compared with the case when δ_p=7 mm. This reduction can be attributed to the diminished effects of impact as the impact gap increases.

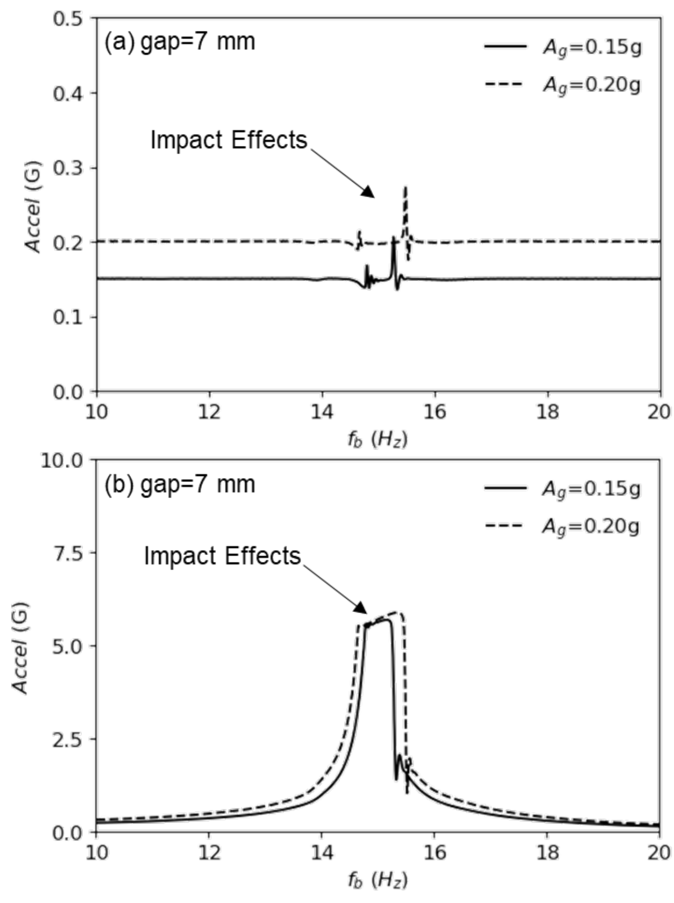

Figure 12: Acceleration plotted in terms of the excitation frequency with impact, comparing the response for the peak accelerations 0.15g and 0.20g: (a) Sensor 1; (b) Sensor 2

Figure 12a and Figure 12b shows the peak values of the acceleration signals recorded by sensors 1 and 2, respectively, plotted in terms of frequency for δ_p=7 mm. Here, sensor 1 is used to regulate vibration levels through the controller and driver. Near the resonance frequency, where the impact occurs, the acceleration shows a sharp change. Following this, the controller manages the sudden shift, ensuring it remains within the specified limits. However, it should be noted that this may affect the performance of the measurement system if the harvester is kept under a base excitation at this resonant frequency. A high-frequency rate is necessary to capture the change while keeping the signal-to-noise ratio very low. In Figure 12b, which shows the peak values of the acceleration signal recorded by sensor 2, a linear increase in acceleration is observed, which is consistent with the previously noted linear increase in voltage during the impact.

7. Conclusions

In this study, an electromagnetic energy harvester was designed, fabricated, and tested for wideband electrical power generation. The harvester utilizes nonlinear dynamics and impact effects induced by a mechanical stopper to enhance its energy generation performance. A theoretical model was developed to predict the induced voltage under measured acceleration signals obtained from a finite element model of a multi-span beam subjected to the dynamic load of a series of moving railcars. This theoretical model accounts for both impact and non-impact scenarios. An experimental study was conducted to assess the impact effects on the performance of a fabricated prototype of the energy harvester. The results demonstrated that the energy harvester's efficiency improves with impact occurrence which led to a bandwidth expansion of 1 Hz when the excitation level reaches 0.20g and the impact gap is set at 7 mm. Furthermore, the maximum output voltage was measured at approximately 43 mV. The study also examined the influence of the impact of gap size on the bandwidth expansion. It was found that increasing the impact gap from 7 mm to 12 mm reduced the maximum output voltage by nearly 15 mV at an excitation level of 0.15g with no improvement in the frequency bandwidth. This highlights the critical role of impact in widening the operational frequency bandwidth, particularly when the impact gap is smaller. Future work should explore the effects of mutli-resonators and impact on the electromagnetic coupling coefficient to develop a more practical model for electromechanical coupling between the moving coil and stationary magnets.

8. References

Aboulfotoh, Noha A., Mustafa H. Arafa, and Said M. Megahed. 2013. "A Self-Tuning Resonator for Vibration Energy Harvesting." *Sensors and Actuators A: Physical* 201:328–34. doi:10.1016/j.sna.2013.07.030.

Ahmad, Muhammad Masood, Nadia Masood Khan, and Farid Ullah Khan. 2021. "Review of Frequency Up-Conversion Vibration Energy Harvesters Using Impact and Plucking Mechanism." *International Journal of Energy Research* 45(11):15609–45. doi:10.1002/er.6832.

Amjadian, M., A. K. Agrawal, and H. Nassif. 2021. "Feasibility of Using a High-Power Electromagnetic Energy Harvester to Power Structural Health Monitoring Sensors and Systems in Transportation Infrastructures." in *Proceedings of SPIE - The International Society for Optical Engineering*. Vol. 11591.

Amjadian, Mohsen, Anil K. Agrawal, and Hani H. Nassif. 2022. "Development of An Analytical Method for Design of Electromagnetic Energy Harvesters with Planar Magnetic Arrays." *Energies* 15(10):3540. doi:10.3390/en15103540.

Amjadian, Mohsen, Anil K. Agrawal, Christian E. Silva, and Shirley J. Dyke. 2022. "Experimental Testing and Validation of the Dynamic Model of a Magneto-Solid Damper for Vibration Control." *Mechanical Systems and Signal Processing* 166:108479. doi:10.1016/J.YMSSP.2021.108479.

Amjadian, Mohsen, and Anil Kumar Agrawal. 2017. "A Passive Electromagnetic Eddy Current Friction Damper (PEMECFD): Theoretical and Analytical Modeling." *Structural Control and Health Monitoring* 24(10):e1978. doi:10.1002/stc.1978.

Bosso, N., M. Magelli, and N. Zampieri. 2021. "Application of Low-Power Energy Harvesting Solutions in the Railway Field: A Review." *Vehicle System Dynamics* 59(6):841–71. doi:10.1080/00423114.2020.1726973.

COMSOL v.5.4. 2024. "Multiphysics® Modeling Software v.6.2."

Dal Bo, L., P. Gardonio, and E. Turco. 2020. "Analysis and Scaling Study of Vibration Energy Harvesting with Reactive Electromagnetic and Piezoelectric Transducers." *Journal of Sound and Vibration* 484:115510. doi:10.1016/j.jsv.2020.115510.

Frýba, Ladislav. 1972. *Vibration of Solids and Structures under Moving Loads*. Dordrecht: Springer Netherlands.

Gao, Mingyuan, Yunwu Li, Jun Lu, Yifeng Wang, Ping Wang, and Li Wang. 2018. "Condition Monitoring of Urban Rail Transit by Local Energy Harvesting." *International Journal of Distributed Sensor Networks* 14(11):1550147718814469. doi:10.1177/1550147718814469.

Hadas, Zdenek, Ondrej Rubes, Filip Ksica, and Jan Chalupa. 2022. "Kinetic Electromagnetic Energy Harvester for Railway Applications—Development and Test with Wireless Sensor." *Sensors (Basel, Switzerland)* 22(3):905. doi:10.3390/s22030905.

Halim, Miah A., and Jae Y. Park. 2014. "Theoretical Modeling and Analysis of Mechanical Impact Driven and Frequency Up-Converted Piezoelectric Energy Harvester for Low-Frequency and Wide-Bandwidth Operation." *Sensors and Actuators A: Physical* 208:56–65. doi:10.1016/j.sna.2013.12.033.

Harne, Ryan L. 2012. "Theoretical Investigations of Energy Harvesting Efficiency from Structural Vibrations Using Piezoelectric and Electromagnetic Oscillators." *The Journal of the Acoustical Society of America* 132(1):162–72. doi:10.1121/1.4725765.

Lu, Yong, Lei Mao, and Peter Woodward. 2012. "Frequency Characteristics of Railway Bridge Response to Moving Trains with Consideration of Train Mass." *Engineering Structures* 42:9–22. doi:10.1016/j.engstruct.2012.04.007.

Malla, Ramesh B., David Jacobs, Suvash Dhakal, and Surendra Baniya. 2017. *Dynamic Impact Factors on Existing Long Span Truss Railroad Bridges*. Rail Safety IDEA Project 25. Transportation Research Board. https://trid.trb.org/view/1479270.

Mann, B. P., and N. D. Sims. 2009. "Energy Harvesting from the Nonlinear Oscillations of Magnetic Levitation." *Journal of Sound and Vibration* 319(1):515–30. doi:10.1016/j.jsv.2008.06.011.

Ouakad, Hassen M., Majid Al-Harthi, and Issam B. Bahadur. 2022. "On the Use of Nonlinear Impact Oscillators in Vibrating Electromagnetic Based Energy Harvesters." *Journal of Intelligent Material Systems and Structures* 33(13):1654–62. doi:10.1177/1045389X211063943.

Pan, Yu, Lei Zuo, and Mehdi Ahmadian. 2022. "A Half-Wave Electromagnetic Energy-Harvesting Tie towards Safe and Intelligent Rail Transportation." *Applied Energy* 313:118844. doi:10.1016/j.apenergy.2022.118844.

Priya, Shashank, and Daniel J. Inman. 2009. *Energy Harvesting Technologies*. Springer US.

Roundy, Shad, Paul Kenneth Wright, and Jan M. Rabaey. 2004. *Energy Scavenging for Wireless Sensor Networks*. Springer US.

Shan, Guansong, Yang Kuang, and Meiling Zhu. 2022. “Design, Modelling and Testing of a Compact Piezoelectric Transducer for Railway Track Vibration Energy Harvesting.” *Sensors and Actuators A: Physical* 347:113980. doi:10.1016/j.sna.2022.113980.

Spreemann, Dirk, and Yiannos Manoli. 2012. *Electromagnetic Vibration Energy Harvesting Devices: Architectures, Design, Modeling and Optimization*. Springer Science & Business Media.

Sun, Yuhua, Ping Wang, Jun Lu, Jingmang Xu, Peigen Wang, Shouyong Xie, Yunwu Li, Jun Dai, Bowen Wang, and Mingyuan Gao. 2021. “Rail Corrugation Inspection by a Self-Contained Triple-Repellent Electromagnetic Energy Harvesting System.” *Applied Energy* 286:116512. doi:10.1016/j.apenergy.2021.116512.

Tang, Lihua, Yaowen Yang, and Chee Kiong Soh. 2010. “Toward Broadband Vibration-Based Energy Harvesting.” *Journal of Intelligent Material Systems and Structures* 21(18):1867–97. doi:10.1177/1045389X10390249.

Wang, Xu, Sabu John, Simon Watkins, Xinghuo Yu, Han Xiao, Xingyu Liang, and Haiqiao Wei. 2015. “Similarity and Duality of Electromagnetic and Piezoelectric Vibration Energy Harvesters.” *Mechanical Systems and Signal Processing* 52–53:672–84. doi:10.1016/j.ymssp.2014.07.007.

Wang, Yifeng, Shoutai Li, Peigen Wang, Mingyuan Gao, Huajiang Ouyang, Qing He, and Ping Wang. 2021. “A Multifunctional Electromagnetic Device for Vibration Energy Harvesting and Rail Corrugation Sensing.” *Smart Materials and Structures* 30(12):125012. doi:10.1088/1361-665X/ac31c5.

Williams, C. B., and R. B. Yates. 1996. “Analysis of a Micro-Electric Generator for Microsystems.” *Sensors and Actuators A: Physical* 52(1):8–11. doi:10.1016/0924-4247(96)80118-X.

Xu, Zhenlong, Wen Wang, Jin Xie, Zhonggui Xu, Maoying Zhou, and Hong Yang. 2017. “An Impact-Based Frequency Up-Converting Hybrid Vibration Energy Harvester for Low Frequency Application.” *Energies* 10(11):1761. doi:10.3390/en10111761.

Yang, Fan, Mingyuan Gao, Ping Wang, Jianyong Zuo, Jun Dai, and Jianli Cong. 2021. “Efficient Piezoelectric Harvester for Random Broadband Vibration of Rail.” *Energy* 218:119559. doi:10.1016/j.energy.2020.119559.

Yang, Y. B., K. Shi, Zhi-Lu Wang, Hao Xu, and Y. T. Wu. 2021. “Theoretical Study on a Dual-Beam Model for Detection of Track/Bridge Frequencies and Track Modulus by a Moving Vehicle.” *Engineering Structures* 244:112726. doi:10.1016/j.engstruct.2021.112726.

Zhu, Dibin, Michael J. Tudor, and Stephen P. Beeby. 2009. “Strategies for Increasing the Operating Frequency Range of Vibration Energy Harvesters: A Review.” *Measurement Science and Technology* 21(2):022001. doi:10.1088/0957-0233/21/2/022001.

Zorlu, Özge, Emre Tan Topal, and Haluk Külah. 2011. “A Vibration-Based Electromagnetic Energy Harvester Using Mechanical Frequency Up-Conversion Method.” *IEEE Sensors Journal* 11(2):481–88. doi:10.1109/JSEN.2010.2059007.